COBEM 2023
27TH INTERNATIONAL CONGRESS OF MECHANICAL ENGENEERING

ABCM
Brazilian Society of Mechanical Sciences and Engineering
27th ABCM International Congress of Mechanical Engineering
December 04-08, 2023, Florianópolis-SC, Brazil

COB-2023-0911
Magnetic instability induced by a current-carrying wire of ferrofluids confined in a Hele-Shaw cell

Fabiano E. Carlos
Rafael M. Oliveira
Departamento de Engenharia Mecânica, Pontífica Universidade Católica do Rio de janeiro, Rio de Janeiro, 22451-900 Brazil
87fabiano@gmail.com
rmo@puc-rio.br

Abstract. *We employ numerical simulations to calculate the shape of the interface separating a nonmagnetic fluid droplet surrounded by a ferrofluid confined in a Hele-Shaw cell. The system is subjected to an azimuthal magnetic field generated by a current-carrying wire. The azimuthal field has a destabilizing effect on the interface and pulls the ferrofluid radially inwards. On the other hand, surface tension tends to stabilize interface deformations. The resulting dynamic behavior and morphological shapes are also influenced by the viscosities of both fluids and the magnetic susceptibility of the ferrofluid. In the current work, we employ an accurate boundary integral method based on the vortex-sheet formalism to examine the nonlinear dynamics and determine these interfacial deformations. For the case in which both nonmagnetic and magnetic fluids have the same viscosities, we analyze how the interplay between magnetic effects and surface tension affect the morphology of the interface. We also investigate the influence of different magnetization responses of the magnetic fluid on pattern formation.*

Keywords: *Numerical Simulation, Magnetic field gradient, Hele-Shaw cell, Ferrofluid.*

1. INTRODUCTION

Rosensweig (1985) and Blums *et al.* (1997) define ferrofluids as stable colloidal suspensions of nanometersized magnetic particles suspended in a nonmagnetic carrier fluid. These magnetic fluids have Newtonian viscosities when subjected to moderate magnetic field intensities and behave superparamagnetically, having a prompt response to an applied external field. As a result, these materials can be easily manipulated by magnetic means. Because of their unique features, Oliveira and Miranda (2020) indicate that ferrofluids have attracted increasing interest in various scientific research areas including physics, chemistry, engineering, material science, biology, and medicine. Torres-Díaz and Rinaldi (2014) and Zhang *et al.* (2019) inform that ferrofluids have been largely used as liquid seals and lubricants held in place by magnetic fields since their development in the 1960s, while interaction with dynamic magnetic fields permitted the manufacturing of ferrofluid-based pumps, valves, and adjustable optical systems. In the field of petroleum engineering, Wang (2021) studied the heating process of an electromagnetic dewaxing system in a pipeline with wax deposition. In this flow assurance problem, the ferrofluid is added as a thin annular layer to the construction of an oil pipeline. Then, a solenoid inside a pig could generate a variable magnetic field which causes movement of the magnetic particles. This in turn leads to heating and facilitate dewaxing.

The addition of magnetic body forces to the equations of fluid mechanics enriches the dynamics of these materials. As a result, it is important to understand how magnetic materials respond to the application of different magnetic field configurations. In addition, the convenient combination of the fluidity of liquids and the magnetic properties of solids makes ferrofluids ideal materials to study a variety of interfacial instabilities and pattern formation processes. As such, the formation of interfacial patterns in ferrofluids when subjected to an external magnetic field has been studied by several researchers. One of the examples, shown in Cowley and Rosensweig (1967), Friedrichs and Engel (2001), Chen *et al.* (2008), and Torres-Díaz and Rinaldi (2014), is the Rosensweig instability. It is formed by the action of a uniform magnetic field applied perpendicularly to ferrofluids resting on a surface and leads to the development of an array of peaks, which results from the combined effects of magnetic, gravitational, and surface tension forces. Interestingly, if the ferrofluid droplet is trapped between the two flat, parallel glass plates of a Hele-Shaw cell, application of the same perpendicular magnetic field configuration leads to the formation of labyrinthine instability patterns (Zahn and Shumovich (1985), Chen *et al.* (2008), and Tsebers and Maiorov (1980)), formed by convoluted multiple branches.

The interfacial patterns observed are very sensitive to the external field and the influence of other magnetic field configurations have been considered in the dynamic deformations of ferrofluid droplets confined in a Hele-Shaw cell. Oliveira and Miranda (2020) considered a simple variation of the previous problem. The perpendicular magnetic field to induce the labyrinthine patterns is generated by two Helmholtz coils with electric currents in the same direction. By keeping the Hele-Shaw half-distance between the coils, and by simply reversing the direction of the electric current

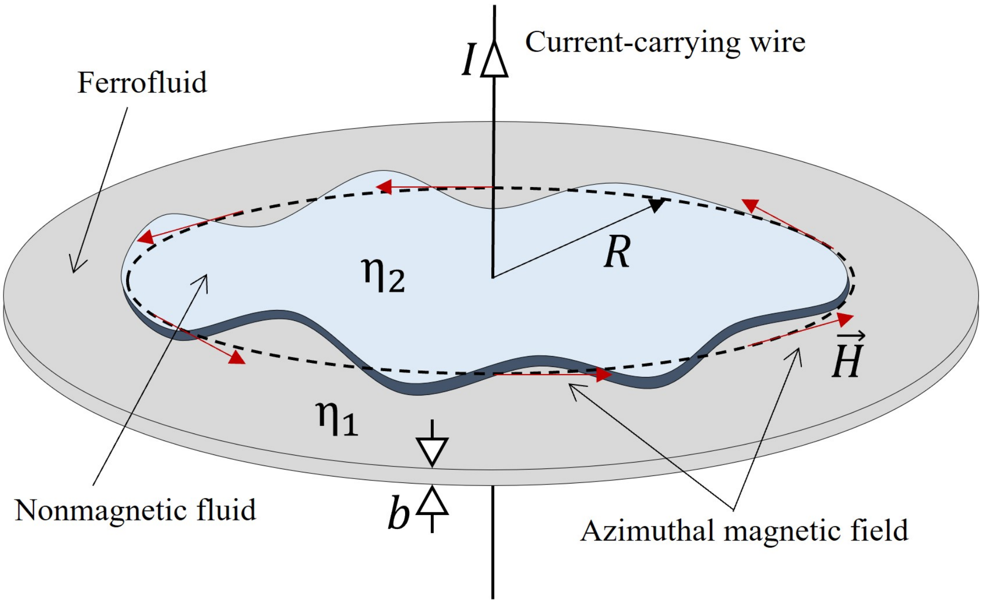

Figure 1. Schematic representation of a nonmagnetic droplet of viscosity η_2, surrounded by a ferrofluid of viscosity η_1, confined between the plates of a Hele-Shaw cell of gap thickness b. The system is subjected to an azimuthal magnetic field H generated by a current-carrying wire with an electric current I.

in one of these coils, the magnetic field on the Hele-Shaw surface becomes in-plane and grows radially. This radial magnetic field when applied to a magnetic droplet leads to interfacial patterns that are strinkingly different from the ones generated by the uniform field. It stretches the droplet radially leading to spiky fingers. Oliveira *et al.* (2021) extended these results by submitting the ferrofluid droplet to crossed magnetic fields, combining an azimuthal field generated by a current-carrying wire with the radial magnetic field. The coupling between the two field configurations led to the formation of skewed sharp fingers that rotate as the pattern stretches. Moreover, Jackson and Miranda (2003) and Lira and Miranda (2010) analyzed the response of a magnetic droplet surrounded by a nonmagnetic fluid in a rotating cell subjected only to the azimuthal magnetic field. In this configuration, the centrifugal forces are the driving mechanism of interfacial instabilities, while the magnetic field and surface tension effects tend to stabilize droplet deformations. Interestingly, by reversing the order of the fluids and considering a nonmagnetic droplet inside the ferrofluid, the azimuthal field becomes the destabilizing agent. Dias and Miranda (2015) have conducted linear and weakly nonlinear analysis of this configuration, while Chen and Lin (2016) conducted nonlinear simulations based on a diffuse-interface approach. The current work expands the analysis initiated by Dias and Miranda (2015) and Chen and Lin (2016) and performs numerical simulations based on a boundary integral method for the case in which both fluids have the same viscosity. We investigate how the interplay between the azimuthal field, the magnetic susceptibility and the surface tension contribute to pattern formation. Experimentally, deformations of nonmagnetic droplets inside a ferrofluids have been explored by Harischandra *et al.* (2023). They fabricate shape-programmed thin films at the air-ferrofluid interface.

The rest of this work is organized as follows. In Sec. 2 we present the governing equations of the system and the vortex sheet formalism, as well as our boundary integral method. In Sec. 3 we analyze how the interplay between magnetic effects and surface tension affects the morphology of the interface for the case in which both nonmagnetic and magnetic fluids have the same viscosities. We also investigate the influence of different magnetization responses of the magnetic fluid on pattern formation. Finally, in Sec. 4 we summarize our findings.

2. PHYSICAL PROBLEM AND GOVERNING EQUATIONS

The physical problem is configured as illustrated in “Fig. 1” with two incompressible and Newtonian fluids. It shows a Hele-Shaw cell of gap thickness b, containing an initially circular droplet of nonmagnetic fluid of radius R and viscosity η_2, surrounded by a ferrofluid of viscosity η_1. The surface tension between them is denoted by σ. A long wire passes perpendicularly through the center of the droplet and carries an electric current I that produces an azimuthal magnetic field of magnitude H in the Hele-Shaw cell plane, as explained in Rosensweig (1985), Miranda (2000), and Lira and Miranda (2010). The azimuthal field destabilizes the two-fluid interface, deforming the circle that has a small initial random perturbation. This perturbation, also applied for Oliveira *et al.* (2023), is built from the superposition of 30 azimuthal Fourier modes

$$(x(\alpha,0), y(\alpha,0)) = R(\alpha)(\cos\alpha, \sin\alpha) \quad (1)$$

with

$$R(\alpha) = 1 + 0.001 \sum_{n=0}^{30} \cos(n\alpha + \phi_n) \tag{2}$$

where ϕ_n is a random phase.

The dynamics of the interface for the geometry of the Hele-Shaw cell is governed by a modified Darcy's law (Tsebers and Maiorov, 1980), which includes the magnetic effect applied in Oliveira and Miranda (2020) and Dias and Miranda (2015) for the gap-averaged velocity,

$$\vec{v_i} = -\frac{b^2}{12\eta_i} \nabla \left(p_i - \frac{1}{2}\mu_0 \chi H^2 \right), \tag{3}$$

where the subscript $i = 1$ for the external ferrofluid and $i = 2$ for the nonmagnetic fluid droplet, and b is the gap of Hele-Shaw cell. The velocity in the bulk of each fluid is given by $\vec{v_i}$, and the pressure is p_i. μ_0 expresses the permeability of free space, χ is ferrofluid's magnetic susceptibility ($\vec{M} = \chi \vec{H}$), $\vec{M}$ being the magnetization of the ferrofluid and $\vec{H} = (1/2\pi r)\hat{e}_\gamma$ being the radial magnetic field strength, where $\hat{e}_\gamma$ indicates the unit vector in the azimuthal direction. This linear magnetization relation holds in the limit of relatively low magnetic field intensities, and if the volume fraction of the nanometersized magnetic particles is not too high.

Two boundary conditions needs to be applied at the interface between the fluids. The kinematic boundary condition states that the normal component of the fluids velocities are continuous across the interface. The second condition is specified by the augmented pressure jump Young–Laplace boundary condition, as described by Rosensweig (1985), Blums *et al.* (1997), and Oliveira and Miranda (2020) and given by

$$p_1 - p_2 = -\left[\sigma\kappa + \frac{1}{2}\mu_0 \left(\vec{M} \cdot \hat{n} \right)^2 \right]. \tag{4}$$

This condition includes the traditional contribution related to surface tension σ and curvature κ, and the magnetic normal traction, which considers the influence of the normal component of the magnetization of the ferrofluid, $\vec{M}$.

To evaluate the fully nonlinear stages of this system's dynamics, we apply the vortex sheet formalism, $\Gamma = (\vec{v_1} - \vec{v_2}) \cdot \hat{s}$, that enables the accurate numerical simulation in time, and explores the jump in the tangential component of the fluid velocity between the ferrofluid (fluid 1) and the nonmagnetic droplet (fluid 2), where $\hat{s}$ represents the unit vector in the arclength direction. The vortex sheet is coupled to evolution equations as described by Oliveira and Miranda (2020), Oliveira *et al.* (2021) and Oliveira *et al.* (2023) and reads

$$\Gamma = -2A\vec{v} \cdot \hat{s} + \nabla \left\{ 2B\kappa + \frac{\chi}{r^2} \left[1 + \chi \left(\hat{n} \cdot \hat{e}_\gamma \right)^2 \right] \right\}, \tag{5}$$

where A is the viscosity contrast and B the effective surface tension, which relates the influences of surface tension with the magnitude of the magnetic field. These two dimensionless parameters are given by

$$A = \frac{\eta_1 - \eta_2}{\eta_1 + \eta_2} \quad \text{and} \quad B = \frac{4\pi^2 \sigma R}{\mu_0 I^2}. \tag{6}$$

These parameters, alongside the magnetic susceptibility, χ, complete the three dimensionless parameters that control the dynamics. In this work, we consider the case in which both fluids have the same viscosity and fix $A = 0$. Next section discusses the influences of χ and B on pattern formation for this limiting case.

3. SIMULATION RESULTS

In this section, we begin our discussion by analyzing in "Fig. 2" the interfacial patterns generated by the destabilization of the azimuthal magnetic field. Because of the $1/r$ dependence of the magnetic field, its magnitude increases as one approaches the origin. It pulls the ferrofluid radially inwards toward the origin of the coordinate system where the current-carrying wire is located. This has a strong influence on the pattern forming structures, and a single, fast growing invading finger is observed in all cases. This can be understood by considering a fast Fourier mode growing from an azimuthal location where the initial perturbation is relatively large. This general condition is found for all cases regardless of the values of the parameters A, B, and χ, and sets the ideal conditions for a fast growing finger that dominates the race towards the origin. As a result, a single, large amplitude invading finger is observed in each simulation. Our analysis is conducted by keeping both fluids with the same viscosity, $A = 0$, and by analyzing the influence of the two remaining governing parameters of the system: the ferrofluid's magnetic susceptibility, χ, and the effective surface tension, B. χ is constant along different columns: (a), (d) and (g) $\chi = 0.1$; (b), (e) and (h) $\chi = 0.25$; and (c), (f) and (i) $\chi = 0.5$. B is constant along different rows: (a)–(c) $B = 0.0005$, (d)–(f) $B = 0.001$, and (g)–(i) $B = 0.0025$. Each image shows the

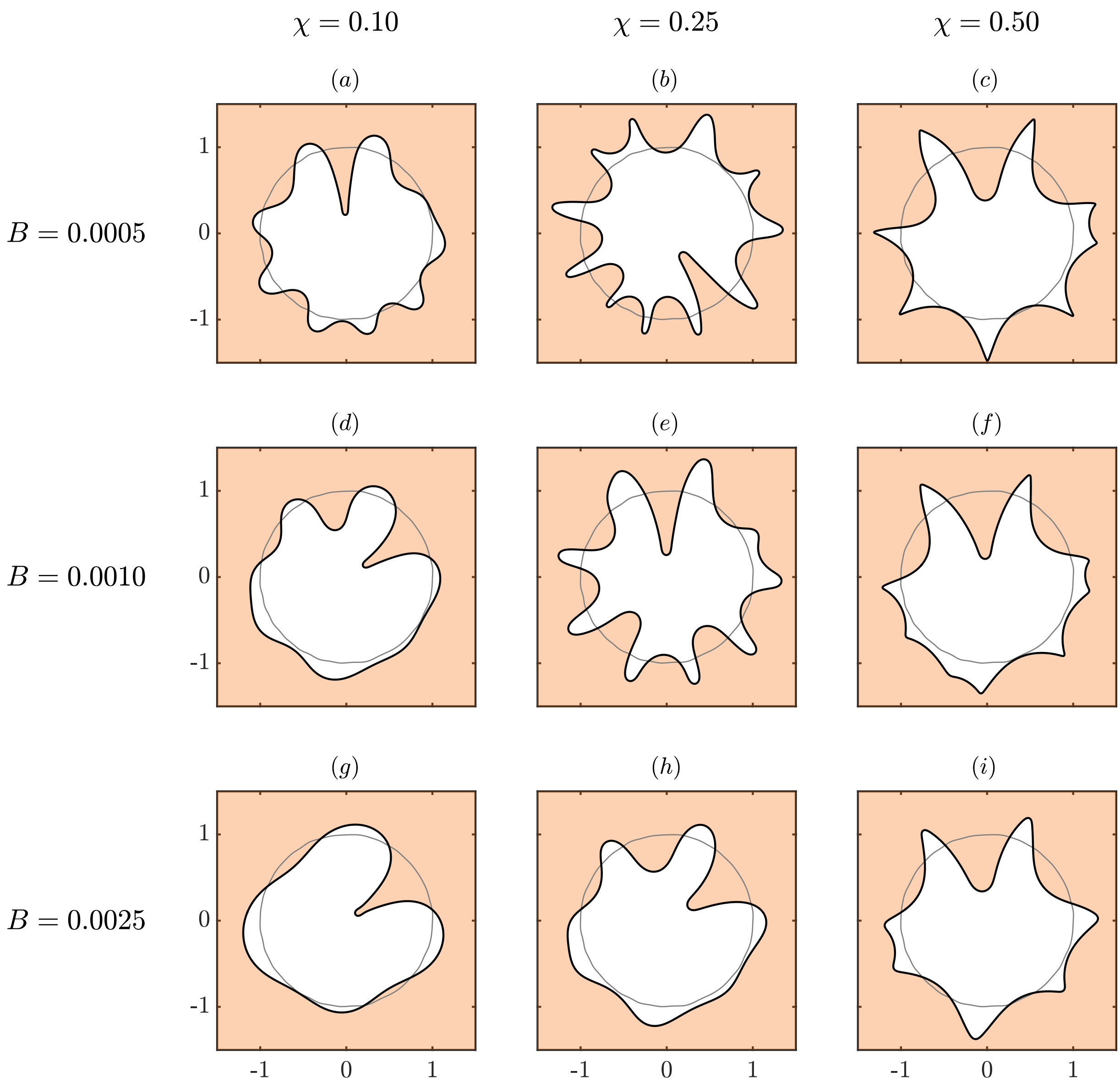

Figure 2. Simulation results. χ is constant along different columns: (a), (d) and (g) $\chi = 0.1$, (b), (e) and (h) $\chi = 0.25$, and (c), (f) and (i) $\chi = 0.5$. B is constant along different rows: (a)–(c) $B = 0.0005$, (d)–(f) $B = 0.001$, and (g)–(i) $B = 0.0025$. The final times, t_f, are (a) 8.3, (b) 3.2, (c) 2.2, (d) 11.27, (e) 3.95, (f) 2.09, (g) 8.69, (h) 4.79, and (i) 2.34.

initial conditions by a slightly perturbed circle of radius $R = 1$ painted in gray and the final simulation times, t_f, that have thick black contours with white interiors to mark the nonmagnetic fluid and is color painted in the exterior to indicate the ferrofluid. The final times are (a) 8.3, (b) 3.2, (c) 2.2, (d) 11.27, (e) 3.95, (f) 2.09, (g) 8.69, (h) 4.79, and (i) 2.34.

From the examination of "Fig. 2", we seek to understand the role played by the effective surface tension B and the magnetic susceptibility χ. By comparing the evolution of initial droplets for different values of B and χ, we can observe the impact of the various simulated ferrofluid shapes and some morphological tendencies. Larger values of B increase the stability of the system regarding the fully nonlinear pattern morphodynamics of the nonmagnetic droplet immersed in the ferrofluid. This tendency is observed through a reduced number of ramifications seen when going down to different rows in the same column. This can be seen by comparing Figs. $2(a) - (c)$, with $2(d) - (f)$, and finally with $2(g) - (i)$. This stabilizing trend is expected because larger values of B indicate a larger relative influence of the surface tension σ. Experimentally, this can be accomplished by reducing the amperage on the current-carrying wire, which increases B-values by lowering the values of the electric current I.

On the other side, the opposite effect occurs when we analyze the increase of the magnetic susceptibility χ. A stronger magnetic response of the ferrofluid to the applied field leads to the formation of more unstable patterns. We can observe this effect as we move along each row. Consider, for example the set given by Figs. $2(g)$, $2(h)$ and $2(i)$. This set of patterns appears with larger number of ramifications. In addition, the shape of the fingers becomes sharper for larger values of χ. Finally, the time required to obtain the final times are smaller for larger χ-values. This indicates a faster evolution of the pattern-forming structures corroborating the unstable nature of the parameter. Notice that the observations regarding faster growth and shaper fingers are common to all rows. However, the number of ramifications in Fig. $2(c)$ is smaller than $2(b)$. Having the smallest B and the larger χ value investigated, Fig. $2(c)$ is expected to be most unstable case. Its finger tips are quite sharp, and the the fast evolution seems to prevent the formation of tip splittings so the number of ramifications are not so severe as the one in Fig. $2(b)$.

4. CONCLUSIONS AND PERSPECTIVES

In this work, we studied the fully nonlinear dynamics of a non magnetic droplet encircled by a ferrofluid in a Hele-Shaw cell. A current-carrying wire passing through the center of the nonmagnetic droplet generates an azimuthal magnetic field that induces an radial magnetic force that pull the external ferrofluid towards the wire. The performed numerical simulations are based on a boundary integral method that uses a vortex sheet formalism to track interfacial evolution and describe pattern formation. By keeping both fluids with the same viscosity, we set the viscosity contrast $A = 0$, and analyzed the effects of the effective surface tension, B, and the ferrofluid's magnetic susceptibility, χ, on the morphology of the nonmagnetic droplet.

Results from numerical simulations show that the an increase in B stabilizes the interface, while χ destibilizes it. This effect can be observed through the formation of pattern-forming structures with sharper fingers pointing in the outward radial direction in Fig. $2(c)$. Our simulations supplement previous theoretical and computational studies of the system initiated by Dias and Miranda (2015) and Chen and Lin (2016). An extension of this work is the study of the impact of viscosity contrast, A, in the deformations of the interface. We expect to observe an interplay of the magnetic-driven instability with the Saffman-Taylor instability associated with viscosity changes. We plan to perform numerical simulations to investigate these phenomena.

5. ACKNOWLEDGEMENTS

We thank CAPES (Coordenação de Aperfeiçoamento de Pessoal de Nível Superior), Brazilian agency, for research support.

6. REFERENCES

Blums, E., Cebers, A. and Maiorov, M.M., 1997. *Magnetic Fluids*. De Gruyter, New York.

Chen, C.Y. and Lin, T.S., 2016. *Interfacial Instability of a Non-magnetized Drop in Ferrofluids Subjected to an Azimuthal Field: A Diffuse-Interface Approach*. Birkhäuser, Maihingen.

Chen, C.Y., Tsai, W.K. and Miranda, J.A., 2008. "Hybrid ferrohydrodynamic instability: Coexisting peak and labyrinthine patterns". *Physical Review E*, Vol. 77, No. 056306.

Cowley, M.D. and Rosensweig, R.E., 1967. "The interfacial stability of a ferromagnetic fluid". *Journal of Fluid Mechanics*, Vol. 30, pp. 671–688.

Dias, E.O. and Miranda, J.A., 2015. "Azimuthal field instability in a confined ferrofluid". *Physical Review E*, Vol. 91, No. 023020.

Friedrichs, R. and Engel, A., 2001. "Pattern and wave number selection in magnetic fluids". *Physical Review E*, Vol. 64, No. 021406.

Harischandra, P.A.D., Välisalmi, T., Cenev, Z.M., Linder, M.B. and Zhou, Q., 2023. "Shaping liquid droplets on an active air-ferrofluid interface". *Langmuir*, Vol. 0, No. 37224278.

Jackson, D.P. and Miranda, J.A., 2003. "Controlling fingering instabilities in rotating ferrofluids". *Physical Review E*, Vol. 67, No. 017301.

Lira, S.A. and Miranda, J.A., 2010. "Stationary shapes of confined rotating magnetic liquid droplets". *Physical Review E*, Vol. 82, No. 036318.

Miranda, J.A., 2000. "Rotating hele-shaw cells with ferrofluids". *Physical Review E*, Vol. 62, No. 2985.

Oliveira, R.M., Abedi, B., Santos, L.F., Câmara, P.S. and Mendes, P.R.S., 2023. "Similarity characteristics in the morphology of radial viscous fingers". *Physics of Fluids*, Vol. 35, No. 042114.

Oliveira, R.M., Coutinho, I.M., Anjos, P.H.A. and Miranda, J.A., 2021. "Shape instabilities in confined ferrofluids under crossed magnetic fields". *Physical Review E*, Vol. 104, No. 065113.

Oliveira, R.M. and Miranda, J.A., 2020. "Fully nonlinear simulations of ferrofluid patterns in a radial magnetic field". *Physical Review Fluids*, Vol. 5, No. 124003.

Rosensweig, R.E., 1985. *Ferrohydrodynamics*. Cambridge University Press, Cambridge, UK.

Torres-Díaz, I. and Rinaldi, C., 2014. "Recent progress in ferrofluids research: novel applications of magnetically controllable and tunable fluids". *Soft Matter*, Vol. 10, No. 8784.

Tsebers, A.O. and Maiorov, M.M., 1980. "Magnetostatic instabilities in plane layers of magnetizable liquids". *Magnetohydrodynamics (N.Y.)*, Vol. 16, No. 21.

Wang, N., 2021. *Ferrouid Applications in Petroleum Engineering*. Ph.D. thesis, The University of Texas at Austin, Austin.

Zahn, M. and Shumovich, R., 1985. "Labyrinthine instability in dielectric fluids". *IEEE Transactions on Industry Applications*, Vol. IA-21, No. 1.

Zhang, X., Sun, L., Yu, Y. and Zhao, Y., 2019. "Flexible ferrofluids: Design and applications". *Adv. Mater*, Vol. 31, No. 1903497.

7. RESPONSIBILITY NOTICE

The authors are solely responsible for the printed material included in this paper.